Open access • Journal Article • DOI:10.1126/SCIENCE.AAF7254

Plant development regulated by cytokinin sinks — Source link

Evelyne Zürcher, Jingchun Liu, Martin Di Donato, Markus Geisler ...+1 more authors

Institutions: University of Zurich, University of Fribourg

Published on: 02 Sep 2016 - Science (American Association for the Advancement of Science)

Topics: Cytokinin transport and Cytokinin

Plant development regulated by cytokinin sinks

Zurcher, E ; Liu, J ; di Donato, M ; Geisler, M ; Muller, B

DOI: https://doi.org/10.1126/science.aaf7254

Title: Plant development regulated by cytokinin sinks

Authors: Evelyne Zürcher[1]†, Jingchun Liu[1]†, Martin di Donato[2], Markus Geisler[2] & Bruno Müller[1]*

Affiliations:

[1]University of Zurich, Department of Plant and Microbial Biology, Zurich-Basel Plant Science Center, 8008 Zurich, Switzerland.

[2]University of Fribourg, Department of Biology, Plant Biology, 1700 Fribourg, Switzerland.

*Correspondence to: bruno.mueller@uzh.ch.

† These authors contributed equally.

Abstract: Morphogenetic signals control patterning of multicellular organisms. Cytokinins are mobile signals that are perceived by subsets of plant cells. Here, we show that the responses to cytokinin signaling during Arabidopsis development are constrained by the transporter PURINE PERMEASE 14 (PUP14). *PUP14* is inversely expressed to the cytokinin signaling readout. The loss of *PUP14* function allows ectopic cytokinin signaling accompanied by aberrant morphogenesis in embryos, roots and the shoot apical meristem. PUP14 protein localizes to the plasma membrane and imports bioactive cytokinins, thus depletes apoplastic cytokinin pools and inhibits perception by plasma-membrane localized cytokinin sensors. We propose that the spatiotemporal cytokinin sink patterns established by PUP14 determine the cytokinin signaling landscape shaping morphogenesis of land plants.

One Sentence Summary: Cytokinin import mediated by Arabidopsis PURINE PERMEASE 14 confines the cytokinin signaling-patterning landscape to control morphogenesis.

Main Text: Multicellular organisms depend on differential cell functions controlled by signaling systems. The precise determination of signal-perceiving cells is important to ensure normal development. Cytokinins are chemical plant signals that control morphogenesis, integrate environmental cues, and mediate biotic interactions (*1–3*). Cytokinins are perceived by largely redundantly acting hybrid kinases that activate a phosphorelay circuitry to stimulate transcription of target genes. The spatiotemporal precision of the signaling patterns in the different plant organs (*4*, *5*) raises the question of how control is established. Each step involved in eliciting a signaling response, including ligand biosynthesis or expression of signaling components, may be differentially regulated and contribute to defining the signaling patterns. To identify limiting and regulated steps, we used Arabidopsis heart-stage embryos as a model where the cytokinin

response marks the provascular tissue (Fig. 1A). First, to evaluate whether bioactive cytokinins are limited, embryos were incubated for 16 h with the degradation-insensitive cytokinin benzyl adenine (BA) (*6*). This caused a stereotypic expansion of the synthetic cytokinin reporter *TCSn::GFP (Two Component signaling Sensor new::green fluorescent protein)* (*5*) (Fig. 1A), confirming that cytokinin levels are controlled (*7*). However, excess cytokinins did not induce *TCSn::GFP* expression in the prospective cotyledons. This is despite the transcription of the cognate cytokinin receptor *ARABIDOPSIS HISTIDINE KINASE 4 (AHK4)* in these domains (Fig. 1A), suggesting that failure to turn on signaling cannot be explained by missing receptors. To test whether signaling downstream of receptors is functional, we expressed *CYTOKININ INDEPENDENT 1 (CKI1)*. *CKI1* encodes a hybrid kinase with cytokinin-independent constitutive activity (*3*). Its short-term expression caused ubiquitous *TCSn::GFP* activation (Fig. 1A). Together, these results suggest that cells of the prospective cotyledons fail to activate cytokinin signaling despite a functional signaling system, and even upon addition of abundant active ligand. We hypothesized that productive ligand-receptor interactions within organs could depend on cytokinin transporters that guide differential cellular localization of cytokinins. To test whether members of the Arabidopsis PURINE PERMEASES (PUPs) family of transmembrane proteins implicated in cytokinin translocation (*8*) control the spatio-temporal landscape of cytokinin signaling, we first established a transcription profile of all family members based on our own analysis and published transcriptome data (*9–11*) (fig. S1). *PUP14* expression was unique to prevail in all organs and stages analyzed, including embryos. To determine the *PUP14* expression pattern, we analyzed *PUP14::PUP14-GFP* transgenic plants. In heart-stage embryos, PUP14-GFP localized to cells that failed to respond to cytokinins including cells of the prospective cotyledons (Fig. 1A). We confirmed this pattern by mRNA in situ hybridization with a *PUP14* antisense probe (Fig. 1B, fig. S2A). The exclusive nature of *PUP14* expression and the cytokinin signaling pattern is compatible with an inhibitory function of PUP14 in the cytokinin response. To eliminate *PUP14* function during defined time windows, which avoids secondary effects and potential lethality issues, we constructed an ethanol-inducible artificial microRNA (*amiR*) (*12*) targeting *PUP14 (35S>ALC>amiRPUP14)*. Upon induction of the *amiRPUP14* transgene, *PUP14* mRNA and PUP14-GFP levels were reduced within 24 h (Fig. 1D, fig. S2, B and C). The *amiRPUP14*-induced phenotypes were complemented by an *amiRPUP14*-resistant transgene *(PUP14*)* encompassing the *PUP14* locus (fig. S2, E to G), suggesting that the inducible *amiRPUP14* acts specifically. In addition, an inducible *amiR* against non-expressed *PUP19* and *PUP20* (fig. S1) did not cause obvious phenotypes (fig. S2, E to G). Finally, a T-DNA insertion to the *PUP14* promoter causing a reduction in *PUP14* mRNA levels showed qualitatively similar but weaker phenotypes in embryos, seedlings and adult shoots compared to *amiRPUP14*-induced phenotypes (Fig. 1C, fig. S3, A to F), while a second T-DNA insertion 3-prime of the *PUP14* locus did not affect *PUP14* mRNA levels (fig. S3B) and produced no apparent phenotypes. Together, these results validate the use of the *amiRPUP14* line to study *PUP14* function. Inducing *amiRPUP14* expression for 16 h caused widespread ectopic cytokinin signaling in the embryo (Fig. 1B), also in cells of the prospective cotyledons that are non-responsive to treatments with exogenous cytokinins (Fig. 1A), supporting the role of PUP14 in confining the cytokinin response. The same treatment regime did not affect the auxin response (fig. S2D), indicating that PUP14 acts specifically on cytokinin signaling. After 2 d of *amiRPUP14* induction, morphological defects in the prospective cotyledons and the nascent root meristem became apparent (Fig. 1B), consistent with the ectopic cytokinin responses in these domains. As loss of *PUP14* produces ectopic cytokinin responses, we expected the

overexpression of *PUP14* to reduce cytokinin output. While we were unable to recover plants transgenic for *35S::PUP14*, inducible *PUP14* expression in the embryo reduced the endogenous cytokinin response after 16 h, and after 48 h of transgene induction, morphological defects in the embryo root were apparent (Fig. 1C). Similar to the embryo, we found *PUP14* expression in the meristematic region of the seedling's main root (fig. S4A), the lateral root primordia (LRP) (fig. S4D), and in ovules and seeds (fig. S5, A and B) exhibiting complementary patterns to those of cytokinin signaling. As in the embryo, short-term *amiRPUP14* induction resulted in ectopic cytokinin signaling in the seedling root, particular in the meristematic region of the root tip (fig. S4A) and in the LRP (fig. S4B). Accordingly, transcription of the immediate-early cytokinin target genes type-A *ARABIDOPSIS RESPONSE REGULATORS (ARR) ARR5*, *6* and *7* (*13*) was induced in seedlings (Fig. 1C). Continuous induction of *amiRPUP14* led to growth retardation of the seedling root and shoot, and a suppression of lateral roots (*14*, *15*) (Fig. 1E), suggesting that the root and shoot meristem activities were both affected when cytokinin signaling patterns were perturbed by the inducible *amiRPUP14*. In contrast to the embryo (Fig. 1B), *TCSn::GFP* expression remained unchanged after 24 h of inducing ectopic *PUP14* in the seedling root (not shown). We visualized PUP14-GFP expressed from the inducible *35S>ALC>PUP14-GFP* transgene and found that, compared to *35S>ALC>GFP*, cells of the root apex and vasculature failed to express PUP14-GFP (fig. S5, A to C) suggesting that ectopic PUP14 is not tolerated, which can explain the absent effects on *TCSn::GFP* in the seedling root apex, and the lethality of the 3*5S::PUP14* transgene. In addition, the subcellular localization of ectopic PUP14-GFP was disturbed compared to endogenous PUP14-GFP (fig. S5, B to C), which may impair its normal function. In the shoot, cytokinin controls the homeostasis of the shoot apical meristem (SAM) (*16*), where increased cytokinin causes a more active meristem with more primordia (*17*). As observed in other developmental contexts (Fig. 1, A to B, figs. S4, S6, A and B), *PUP14* expression in the SAM was inversely correlated with cytokinin signaling output assayed by *TCSn::GFP* (Fig. 2A). Inducing *amiRPUP14* expression in adult plants that were allowed to complete embryogenesis and the early vegetative phase of development undisturbed caused ectopic cytokinin output in the SAM, which was accompanied by a 37% more primordia, 94% increased shoot branching and disturbed phyllotaxis (Fig. 2, B and C). Similar phenotypes have been observed in plants mutant for *CYTOKININ OXIDASE (CKX) 3* and *5* (*17*)*, ARABIDOPSIS HISTIDINE PHOSPHOTRANSFER PROTEIN 6* (*18*), and *ARR3-9* (*19*), which also display ectopic cytokinin activities. Thus, PUP14 functions to limit the cytokinin response domains throughout development to support morphogenesis.

Next, we addressed the cellular function of PUP14. PUP14-GFP fusion proteins, supported by BFA-sensitive vesicular transport, localize to the plasma membrane (fig. S6C). To test PUP14's cytokinin transport capacity, we conducted uptake experiments using labelled trans-zeatin (tZ), an abundant natural cytokinin (*20*). Transient expression of *PUP14* in mesophyll protoplasts or tobacco microsomes stimulated the uptake of labelled tZ (Fig. 3, A and B). The PUP14 transport activity was ATP-dependent and higher compared to PUP1 (*8*) (Fig. 3B). Uptake was inhibited by unlabeled tZ, by the common natural cytokinin isopentenyl adenine (iP), by the aromatic cytokinin BA, and also by adenine, but not by tZ riboside, the major cytokinin transport form (*21*), nor auxin (IAA), nor allantoin, which is an unrelated substrate (Fig. 3, C and D). Energy-dependent cytokinin uptake into a microsomal cell-free system excludes that uptake is dependent on cytoplasmic metabolization. Conversely, seedlings with decreased *PUP14* levels exhibited a reduced uptake rate for exogenously added tZ compared to control seedlings (Fig. 3E).

Our data show that plasma membrane-localized PUP14 imports bioactive cytokinins to the

cytosol, implying that PUP14 activity depletes ligands from the apoplast, which leads to a suppression of the cytokinin response. In this scenario, extracellular cytokinins binding to the sensing domains of plasma membrane-localized receptors (*22*, *23*) are important to initiate the signaling response, while the cytoplasm represents a sink for bioactive ligands. To test this hypothesis, we devised experiments that compare the effects of differentially targeted cytokinin-degrading enzymes on the cytokinin signaling response. Mesophyll protoplast cells responded to as little as 100 pM of exogenously added tZ by activating cytokinin signaling (*4*), suggesting they depend on exogenous cytokinins, and thus serve as a suitable model to study cytokinin perception independent of production. Transient transfection of PUP14 localizing to the plasma membrane (fig. S7A) caused a reduction of cytokinin-dependent *TCS::LUCIFERASE (LUC)* activity (Fig. 3F), recapitulating the phenotypes from *PUP14* overexpression in the embryo (Fig. 1B). Transient expression of wild-type CKX2 that is targeted for secretion to the apoplast (*20*) (fig. S7B) attenuated the cytokinin response triggered by tZ but not by the degradation-resistant BA. To target CKX2 to the exofacial side of the plasma membrane, we added a glycosyl phosphatidyl inositol (GPI)-anchor (*24*) resulting in CKX2-GPI (fig. S7C), which also caused a reduction in the cytokinin response. In contrast, a variant of CKX2 that lacks the N-terminal signal peptide (ΔSP-CKX2) and co-localizes with a cytoplasmic marker (fig. S7D) did not affect the cytokinin response, and neither did CKX7, which also localizes to the cytoplasm (*25*) (fig. S7E). Crude cell extracts obtained from ΔSP-CKX2- or CKX7-transfected cells added to the medium reduced the response triggered by tZ, indicating these proteins are active. These data suggest that apoplastic cytokinins initiate signaling, while cytoplasmic cytokinins are inactive.

PUP14 imports cytokinins from the apoplast to the cytosol, away from sensing domains of plasma membrane-localized receptors, which causes a reduction in cytokinin signaling. Thus, PUP14 activity inversely correlates with the capacity of a cell to sense cytokinins (fig. S8), and PUP14 spatio-temporal activities cause region-specific depletion of cytokinins from the apoplast. In animals, the importance of such clearing activities is demonstrated by the powerful action of drugs that target dopamine influx transporters thereby increasing its residence time in the synaptic cleft (*26*). Feeding experiments with radiolabeled bioactive cytokinin suggested that the bulk of imported cytokinins are inactivated by conversion to monophosphates by ADENINE PHOSPHORIBOSYL TRANSFERASE enzymes (*27*, *28*). Furthermore, N- or O-glycosylation, oxidative cleavage, or transport to other cells may contribute to clearance of intracellular cytokinins (*2*). PUP14 is the only family member to be linked to cytokinin signaling in all organs. In specific developmental contexts, additional PUP family members likely have overlapping functions with PUP14. The fact that *PUP* genes are specific to vascular plants (*29*) may suggest *PUP* genes are needed to support more complex cytokinin signaling patterns associated with the bauplan of land plants. As hormonal transporters are numerous and universal in plant and animal systems, transporters in other systems may also regulate patterning during morphogenesis.

References and Notes:

1. M. Miri, P. Janakirama, M. Held, L. Ross, K. Szczyglowski, *Trends Plant Sci.* **21**, 178 (2016).
2. J. J. Kieber, G. E. Schaller, *Arabidopsis Book* **12**, e0168 (2014).
3. I. Hwang, J. Sheen, B. Müller, *Annu. Rev. Plant Biol.* **63**, 353 (2012).
4. B. Müller, J. Sheen, *Nature* **453**, 1094 (2008).

5. E. Zürcher *et al.*, *Plant Physiol.* **161**, 1066 (2013).
6. P. Galuszka *et al.*, *J Plant Growth Regul* **26**, 255 (2007).
7. B. De Rybel *et al.*, *Science* **345**, 1255215 (2014).
8. B. Gillissen *et al.*, *Plant Cell* **12**, 291 (2000).
9. J. Adrian *et al.*, *Dev. Cell* **33**, 107 (2015).
10. M. F. Belmonte *et al.*, *Proc. Natl. Acad. Sci. U S A* **110**, E435 (2013).
11. R. K. Yadav, M. Tavakkoli, M. Xie, T. Girke, G. V. Reddy, *Dev.* **141**, 2735 (2014).
12. R. Schwab, S. Ossowski, M. Riester, N. Warthmann, D. Weigel, *Plant Cell* **18**, 1121 (2006).
13. I. B. D'Agostino, J. Deruère, J. J. Kieber, *Plant Physiol.* **124**, 1706 (2000).
14. L. Laplaze *et al.*, *Plant Cell* **19**, 3889 (2007).
15. J. P. To *et al.*, *Plant Cell* **16**, 658 (2004).
16. S. P. Gordon, V. S. Chickarmane, C. Ohno, E. M. Meyerowitz, *Proc. Natl. Acad. Sci. U S A* **106**, 16529 (2009).
17. I. Bartrina, E. Otto, M. Strnad, T. Werner, T. Schmülling, *Plant Cell* **23**, 69 (2011).
18. F. Besnard *et al.*, *Nature* **505**, 417 (2014).
19. A. Leibfried *et al.*, *Nature* **438**, 1172 (2005).
20. T. Werner *et al.*, *Plant Cell* **15**, 2532 (2003).
21. C. A. Beveridge *et al.*, *Plant J.* **11**, 339 (1997).
22. H. J. Kim *et al.*, *Proc. Natl. Acad. Sci. U S A* **103**, 814 (2006).
23. K. Wulfetange *et al.*, *Plant Physiol.* **156**, 1808 (2011).
24. A. Baral *et al.*, *Plant Cell* **27**, 1297 (2015).
25. I. Köllmer, O. Novák, M. Strnad, T. Schmülling, T. Werner, *Plant J.* **78**, 359 (2014).
26. R. A. Vaughan, J. D. Foster, *Trends Pharmacol Sci* **34**, 489 (2013).
27. B. Moffatt, C. Pethe, M. Laloue, *Plant Physiol.* **95**, 900 (1991).
28. X. Zhang *et al.*, *Mol Plant* **6**, 1661 (2013).
29. S. B. Hildreth *et al.*, *Proc. Natl. Acad. Sci. U S A* **108**, 18179 (2011).
30. D. R. Smyth, J. L. Bowman, E. M. Meyerowitz, *Plant Cell* **2**, 755 (1990).
31. D. S. Lituiev *et al.*, *Dev.* **140**, 4544 (2013).
32. S. J. Clough, A. F. Bent, *Plant J.* **16**, 735 (1998).
33. H. A. Roslan *et al.*, *Plant J.* **28**, 225 (2001).
34. C. Xiang, P. Han, I. Lutziger, K. Wang, D. J. Oliver, *Plant Mol. Biol.* **40**, 711 (1999).
35. C. Aslanidis, P. J. de Jong, *Nucleic Acids Res.* **18**, 6069 (1990).
36. B. De Rybel *et al.*, *Plant Physiol.* **156**, 1292 (2011).
37. S. D. Yoo, Y. H. Cho, J. Sheen, *Nat Protoc* **2**, 1565 (2007).
38. A. Bielach *et al.*, *Plant Cell* **24**, 3967 (2012).
39. S. Henrichs *et al.*, *EMBO J.* **31**, 2965 (2012).
40. K. J. Livak, T. D. Schmittgen, *Methods* **25**, 402 (2001).
41. G. Jach, E. Binot, S. Frings, K. Luxa, J. Schell, *Plant J.* **28**, 483 (2001).

Acknowledgments: We thank Matthias Philipp for technical assistance, Ioanna Antoniadi and Anja Schmidt for sharing unpublished results, Enrico Martinoia (E.M.) for help with transport assays, Jen Sheen and Konrad Basler for critical discussions and comments on the manuscript, Célia Baroux for comments on the manuscript, and Ueli Grossniklaus for

support. Funding was provided by the Kanton of Zurich, the Swiss National Science Foundation (SNF31003A-149459), and by a Syngenta PhD Fellowship from the Zurich-Basel Plant Science Center. The authors declare that they have no conflicts of interest. The supplementary materials contain additional data. Plasmid sequences were deposited to Genbank, accession numbers are KX510271-KX510275.

Fig. 1. PUP14 function in embryo and seedlings.

(**A**) Heart-stage embryos subjected to 16 h mock, 16 h 10 µM BA treatment, hybridized with *AHK4* antisense (as) RNA, and 16 h *CKI1* expression from a *35S>ALC>CKI1* transgene (*5*) (*CKIox*). GFP reporter transgenes as indicated. (**B**) *PUP14* expression detected by reporter gene and by *PUP14* as RNA probe. *amiRPUP14* and *PUP14* transgene inductions, ectopic *TCSn::GFP* in 85% of embryos, n=53, loss of *TCSn::GFP* in 45% of embryos, n=11. (**C**) Morphological defects 48 h after transgene inductions and in *pup14-1* (for *amiRPUP14* 47%, n=96, for *pup14-1*, 37%, n=237, for *PUP14* overexpression from *35S>ALC>PUP14* [*PUP14ox*], 50%, n=10), (arrowheads point to affected cotyledons, arrow to shortened embryo root, cell boundaries in root meristem outlined with white dotted lines). (**D)** Relative changes of type-A *ARR5*, *6* and *7,* and *TCSn::GFP* (as a group significantly different: $p<0.001$ from unpaired t-test, *TCSn::GFP:* n=4; *TCSn::GFP, amiRPUP14*: n=4) and *PUP14* mRNA levels (significantly different: $p<0.001$ from unpaired t-test, *TCSn::GFP:* n=4; *TCSn::GFP, amiRPUP14*: n=7) after 16 h of *amiRPUP14* induction in 7 d old seedlings of indicated genotype, assessed by quantitated real-time (qRT)-PCR, error bars represent s.e.m. (**E**) Seedlings after 7 d on ethanol-containing medium. Growth retardation of seedling roots, n=10. Scale bars (A to B) 20 µm, (E) 1 cm.

Fig. 2. PUP14 confines the cytokinin response in the SAM.

(**A**) Floral SAM. Longitudinal optical sections in lower panels at cyan-colored brackets, dotted lines mark organ boundaries. Transgenes indicated. Arrows indicate peak *PUP14-GFP* levels at organ-organ boundaries. Ectopic *TCSn::GFP* (arrowheads) after *amiRPUP14* induction. (**B-C**) Comparisons of ethanol-treated Col0 and *amiRPUP14* phenotypes. (**B**) Inflorescences and inflorescence stems, red dots denote flower primordia, arrowheads indicate perturbations. (**C**) Numbers of flower primordia, at stages 6-12 on the main apex (*30*), n=6. Number of primary rosette (RI) and primary cauline branching (CI), n=6. Data represent mean values, error bars represent s.d. **$p < 0.01$ unpaired t-test. Scale bars (A) 20 µm, (B) 1 mm (flower primordia), 1 cm (stems).

Fig. 3. PUP14 cellular function.

(**A-E**) PUP14 transport assays, with relative C14-tZ uptake rates on y-axis. (**A**) *PUP14*-transfected mesophyll protoplasts. (**B**) Microsomes derived from *GFP, PUP1,* or *PUP14* transfected *N. benthamiana*. (**C**) Competition by indicated substances in *PUP14*-transfected protoplasts. (**D**) Competition in microsomes of *35S::PUP14* transfected *N. benthamiana.* (**E**) *amiRPUP14* vs. Col0 seedlings. (**F**) Relative *TCSn::LUC* inductions in protoplasts, treated by 10 nM tZ or BA, co-transfected with effector genes, or addition of cell extracts as indicated, normalized to empty vector

control. Data represent mean values, error bars represent s.d. (A,E) or s.e.m. (B,C,D,F), **p < 0.01, *p <0.05, ANOVA with Tukey's HSD post hoc test.

Supplementary Materials:

Materials and Methods

Figures S1-S8

Tables S1-S2

References (*30-41*)

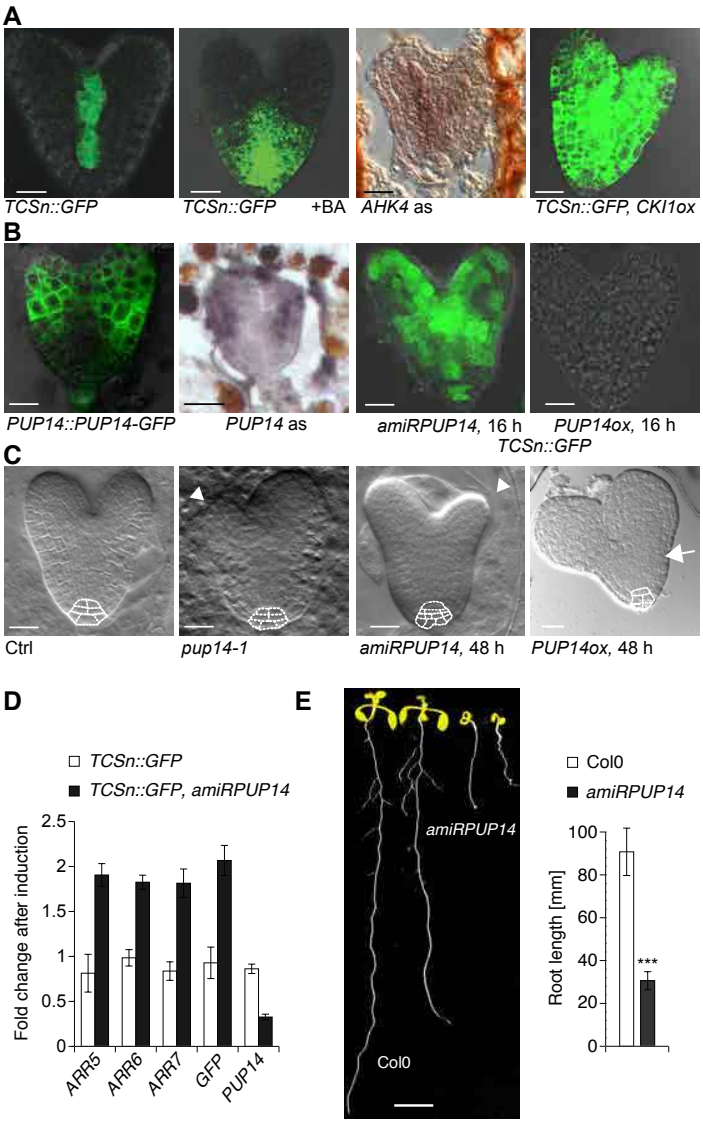

Fig. 1. PUP14 function in embryo and seedlings.

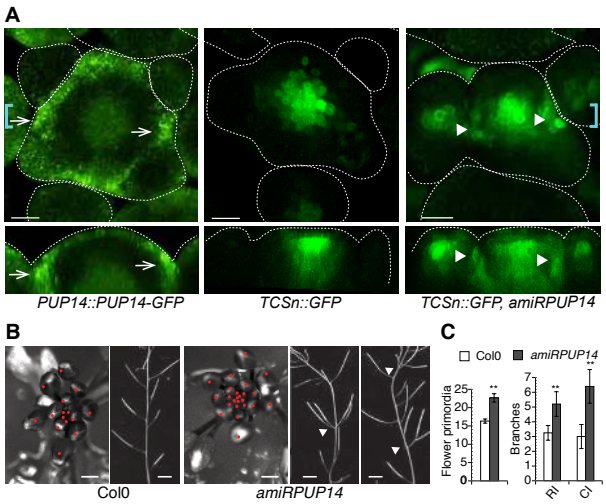

Fig. 2. PUP14 confines the cytokinin response in the SAM.

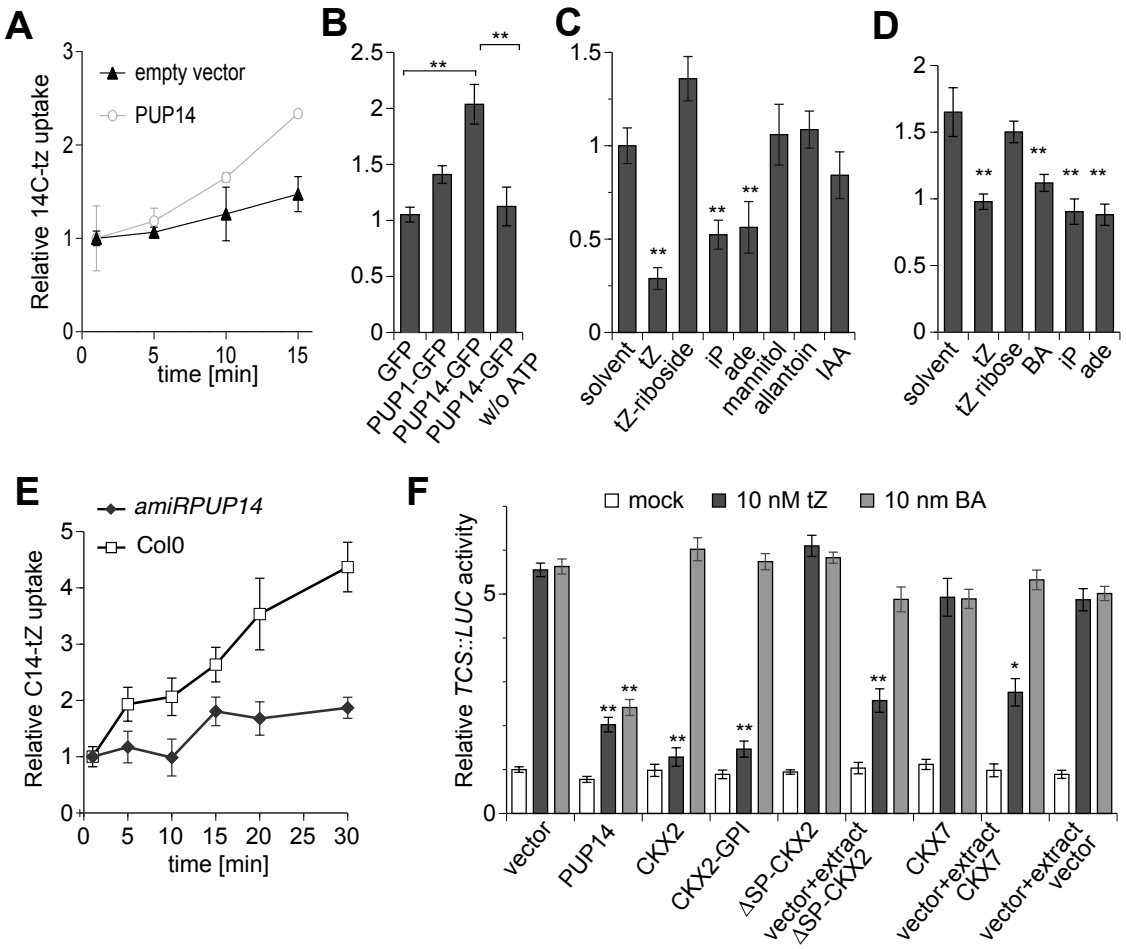

Fig. 3. PUP14 cellular function.

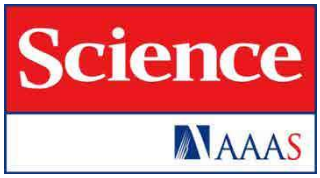

Supplementary Materials for

Plant Development Regulated by Cytokinin Sinks

Evelyne Zürcher, Jingchun Liu, Martin di Donato, Markus Geisler & Bruno Müller
correspondence to: bruno.mueller@uzh.ch

This PDF file includes:

Materials and Methods

Microscopy and live imaging.

RNA in situ hybridization and embryo clearings were observed with a transmission microscope under bright field or differential interference contrast with a 40x lens. For GFP imaging, live embryos or seedlings were mounted in 0.5 strength Murashige and Skoog (MS) liquid medium. SAMs were mounted in warm 0.8% low-gelling agar dissolved in 0.5 strength liquid MS. Confocal microscope observations were done on a SP2 or SP5 spectral detection confocal microscope (Leica) equipped with a 20x glycerol immersion (seedling root, seeds), 40x oil immersion (SAM) or 63x glycerol immersion lens (female gametophytes, embryos). Images were processed using Imaris (Bitplane, Zurich). Maximum partial projections of equivalent serial sections are shown. Fluorescence levels (*TCSn::GFP* and *DR5::tdTomato*) (*31*) were quantified from maximum intensity projections obtained from 6 embryos using ImageJ (http://rsbweb.nih.gov/ij/). Adult plants were recorded with a DP3 Merrill digital camera (Sigma), and flower primordia with a MZFLII fluorescence stereomicroscope equipped with a DFC 420C digital camera (Leica).

Plant material and growth conditions.

The ecotype Col0 was used as wild type. Seeds were surface sterilized for 18 min in 5 % (v/v) bleach and 0.1 % (v/v) triton-X, washed three times in sterile ddH_2O and kept in the dark at 4 °C for a minimum of 2 d for stratification. Seeds were sown on solid medium, containing 0.5 strength MS, 2 % (w/v) sucrose, 0.8 % (w/v) phytagar and 2 mM 2-(N-morpholino)ethanesulfonic acid (MES) pH 5.8, and the appropriate antibiotic or herbicide for selection. Seeds on selection plates were placed into a Percival plant incubator (CU-36L6/D Percival Scientific Inc., Perry IA, USA) with 22 °C and a 14/10 h light/dark regime with 120 mmol m^{-2} s^{-1}. To phenotype seedlings, plants were grown vertically on 12 cm square plates containing 10 mL of medium. To prevent desiccation of the plates, 1 mL of ddH_2O was added and the plates were sealed with parafilm. Seeds on vertical plates were placed into a Percival plant incubator (CU-36L6 Percival Scientific Inc., Perry IA, USA) with 22 °C and 12/12 h light/dark cycles with 90 mmol m^{-2} s^{-1}. To obtain adult plants, seedlings were transferred to soil and grown at 22 °C during the day, 20 °C at night with a 16/8 h photoperiod.

Plant transformation.

Plant transformation was performed using *Agrobacterium tumefaciens* of the GV3101 strain (32). Inducible expression constructs were supertransformed into *TCSn::GFP* or *PUP14::PUP14-GFP* transgenic lines.

Ethanol induction of transgenes

Ethanol was applied as follows to induce expression of *amiRPUP14*, *CKI1*, or *PUP14* from the ethanol-inducible two-component system (*33*). For phenotype assessments of seedlings, 1 mL of 1 % (v/v) ethanol was added to the bottom of the vertical plates 4 d after germination. For expression analyses, 7 d old seedlings grown on vertical plates were transferred to 6-well culture dishes with 3 mL of liquid medium (0.5 strength MS, 2 % (w/v) sucrose, 2 mM MES pH 5.8) with and without 1 % (v/v) ethanol) for 16 - 24 h. Dishes were sealed with parafilm. Induction in adult plants was by watering with 1 % (v/v) ethanol every 4 d starting from bolting stage as described (*33*). Embryo inductions were performed as described (*4*). Controls shown are *TCSn::GFP* treated with ethanol in parallel to the experimental genotypes. Similar results were obtained with untreated *TCSn::GFP, amiRPUP14* plants.

Constructs

For *PUP14::PUP14-GFP*, a DNA fragment encompassing the *PUP14* locus including the 2.3 kb upstream sequence was amplified from Col0 genomic DNA by PCR and cloned into the binary vector pCB302 (34) with the enhanced GFP coding sequence allowing for C-terminal fusions, the nopaline synthase 3-prime untranslated region, and an adaptor for ligation-independent cloning (LIC) (Genbank KX510271) (35). For protoplast experiments, *PUP14*, *CKX2* and *CKX7* genomic regions from translational start to stop were amplified from Col0 genomic DNA and annealed to LIC-modified expression vectors (see Table S2) to yield 2x hemagglutinin (HA) (Genbank KX510274), GFP (Genbank KX510273), or glycosyl phosphatidyl inositol (GPI)-anchored GFP C-terminal translational fusions (Genbank KX510275). *CKX2-GPI* was cloned by restriction digest of *CKX2-2HA* with PstI and StuI and annealing

of oligonucleotides encoding the GPI-anchor. The artificial microRNA (*amiR*) sequences were obtained through the Web MicroRNA Designer (wmd3.weigelworld.org), and assembled by PCR amplification on pRS300 as template as described (12) using LIC-modified primers A and B (see Table S2) to produce fold-back amiR precursors. The fold-back amiR precursors were cloned into the LIC-modified ethanol-inducible binary DM7 vector (5). The sequences of the base-pairing nucleotides of *amiRPUP14_1* and *amiRPUP14_2* are TTATTTGCACAAAGTGTTCTG and TGTTGATAGGTATTTGCACGA, respectively. Both *amiRPUP14* constructs caused similar phenotypes upon induction. Corresponding target sites in *PUP14* are CAGAACAATTTGTGCAAATAC and TTGTGCAAATACCTATCAACA for *amiRPUP14_1* and *amiRPUP14_2*, respectively. Sequence of the base-pairing nucleotides of *amiR19/20* is TTAAAACACGTCCTGCGACGA. Target sequences are TCGTAGCAGGACGTGTTTTAT in *PUP19* and TCGTAACAGGACGTGTTTTAT in *PUP20* amiR-resistant versions of *PUP14* (*PUP14**) were constructed by site-directed mutagenesis of the *amiRPUP14_2* target site to change all codons within the *amiR* target site in *PUP14* to synonymous codons with overall comparable codon usage frequency. The *PUP14** encompasses the *PUP14* genomic region and was cloned into pCB302 by LIC. Inserts for the *35S::PUP1* and *35S::PUP14* binary constructs used for expression in microsomes were amplified from Col0 genomic DNA, and cloned into pPLV26 (36) by LIC. For *PUP14ox*, the *PUP14* translated sequence was amplified from genomic Col0 DNA and ligated into LIC-modified DM7 (5). For *35S>ALC>PUP14-GFP*, *PUP14-GFP* was amplified from *PUP14::PUP14-GFP* and ligated into LIC-modified DM7 (5). All constructs were sequenced to ensure no unwanted mutations were introduced. A plasmid list is provided in Table S2.

Protoplast isolation and transfection

For transient expression experiments, protoplasts of three- to four-week-old wild-type Arabidopsis plants of the Col0 ecotype were isolated as described (*37*) with the following adaptations: adjusted concentration was 3 x 10^5 ml^{-1}, *35S::renillaLUC* was used to normalize for transfection efficiency (*38*) of *TCS::LUC* reporter assays, and WI solution was supplemented with 15 mM sucrose. For reporter assays, transfected protoplasts were incubated over night, DCPIP (2,6-Dichloroindophenol sodium salt hydrate) at 5 µM was added as electron acceptor (*6*), as well as tZ or solvent at indicated concentrations, and protoplasts were harvested 60 min later for LUC measurements. To obtain crude protein extracts, 3 x 10^5 transfected protoplasts were lysed in 200 µl extraction buffer (*6*) with 1.2 % (v/v) plant protease inhibitor mixture (Sigma P9599) and incubated for 5 min at room temperature. The samples were then centrifuged at 21'000 rcf for 5 min at room temperature. Supernatants were transferred to a new tube. 25 µl were added to 3 x 10^4 transfected protoplasts. For transport assays, transfections were scaled up according to needs and purified plasmids were transfected in 1:1 ratio between effector and empty plasmid. Transfected protoplasts were cultivated between 12 and 24 hrs at 22 °C in light (120 mmol m^{-2} s^{-1}). Means and standard error of means of at least two independent experiments with three technical replications each are represented.

In situ hybridizations

mRNA in situ hybridizations were performed as described (*4*). Probe templates for *AHK4* and *PUP14* were synthesized by PCR from Col0 genomic DNA using the following primers: T3_AHK4_f: aattaaccct-cactaaagGATCATCACCCGCAACTCTC, T7_AHK4_r: taatacgactcactatagGATCAACACTGAACCGTC-GTC, T3_PUP14_f: aattaaccctcactaaagATTCTTCAACCACACGCATGAAC, T7_PUP14_r: taatacgactcac-tatagACCAAAGCTGTTACACACTTACAC. T3 and T7 RNA polymerase promoter sequences are indicated in lower case font.

Transport assays

For protoplast transport assays, protoplasts were harvested at 100 rcf for 2 min and re-suspended in percoll solution (0.5 M Sorbitol, 1 mM $CaCl_2$, 20 mM MES pH 5.8, 25 % (v/v) percoll) and mixed with the same volume of glycine betaine solution (0.5 M glycine betaine, 1 mM $CaCl_2$, 20 mM MES pH 5.8) containing ^{14}C- labelled tZ and ^3H_2O. The final concentration of labelled tZ was 1 or 2 µM. For competition studies, unlabeled cold substrate was added in a 100- fold excess. Transport was stopped by centrifugation of samples on a percoll cushion after indicated time points. For scintillation counting, pelleted protoplasts were transferred into 3 mL of Ultima Gold™ (PerkinElmer AG, Schwerzenbach, Switzerland) and subjected to 10 min of disintegration counting of ^{14}C and ^3H. Three independent replicates of the uptake experiment

were conducted with similar results, and means with standard deviations from one representative experiment with four technical replications are shown. For competition assays, mean values from three independent experiments with each four technical replications are shown. Indicated relative uptake was calculated as the radioactivity of ^{14}C per radioactivity of $^{3}H_2O$ normalized to the first time point (30 s). For seedling transport assays, twelve-day old induced seedlings were transferred to liquid medium containing 0.5 MS, 2 % (w/v) sucrose, 2 mM MES and vacuum infiltrated for 5 min and twice 3 min. For each replicate > 10 mg of plant material was used. Radiolabelled tZ was added to a final concentration of 2 µM in 2 mL. Seedlings were washed after indicated time points with excess volumes of cold 0.5 strength MS, 2 % (w/v) sucrose, 2 mM MES on a Büchner funnel. Seedlings were dried on filter paper and transferred to 1.5 ml tubes containing 800 mL of 80 % (v/v) ethanol and heated for 5 min at 95 °C. Samples were transferred into scintillation vials containing 3 mL Ultima Gold™ (PerkinElmer) and subjected to 2 min disintegration counting of ^{14}C. Indicated relative uptake was calculated as the radioactivity per fresh weight normalized to the radioactivity per fresh weight at the first time point (1 min). Mean values from 3 independent experiments with each 4 technical replications are shown. For microsomal uptake experiments, *35S::PUP1*, *35S::PUP14* and *35S::GFP* were transiently expressed in *N. benthamiana* leaf tissue by *Agrobacterium tumefaciens*-mediated transfection and microsomes were prepared as described (*39*). For tZ-uptake experiments, ^{14}C-labelled tZ was diluted into transport buffer (10 mM Tris-HCl, 10 mM $MgCl_2$, 1 mM EDTA, 1 mM DTT, 10 % sucrose, pH 7.6 with or without 5 mM ATP) and added to 300 µg of microsomes to yield a final concentration of 1µM labelled tZ. For substrate competition assays unlabelled substrate was included in the transport buffer at a 100-fold excess. After 10 s and 4 min of incubation at 20 °C, aliquots of 100 µL were vacuum-filtered on Whatman™ NC45 filters (GE Healthcare, Little Chalfont, UK) and washed 3 times with 1 mL cold ddH_2O. Air-dried filters were objected to scintillation counting as described above. Indicated relative uptake was calculated as the radioactivity normalized to the first time point (10 s). Means and standard error of means of at least four independent experiments with three technical replications each are represented.

qRT PCR analysis

Quantification of relative gene expression was done by qRT-PCR on an Applied Biosystems 7500 Fast Real- Time PCR System using SYBR® Green PCR Master Mix (Applied Biosystems, Life Technologies Europe B.V., Zug, Switzerland) or SsoAdvanced™ Universal SYBR® Green Supermix (Bio-Rad Laboratories AG, 1785 Cressier, Switzerland) according to manufacturer's recommendation. Final primer concentrations were 400 nM in a total volume of 20 µl. The relative values of the transcripts were normalized to *EUKARYOTIC TRANSLATION INITIATION FACTOR 4A* (eIF4A, *At3G13920*) levels or to At2G32170. Fold changes were calculated by the $2^{-\Delta\Delta Ct}$ method (*40*). Means and standard error of means of at least three independent experiments with three technical replications each are represented.

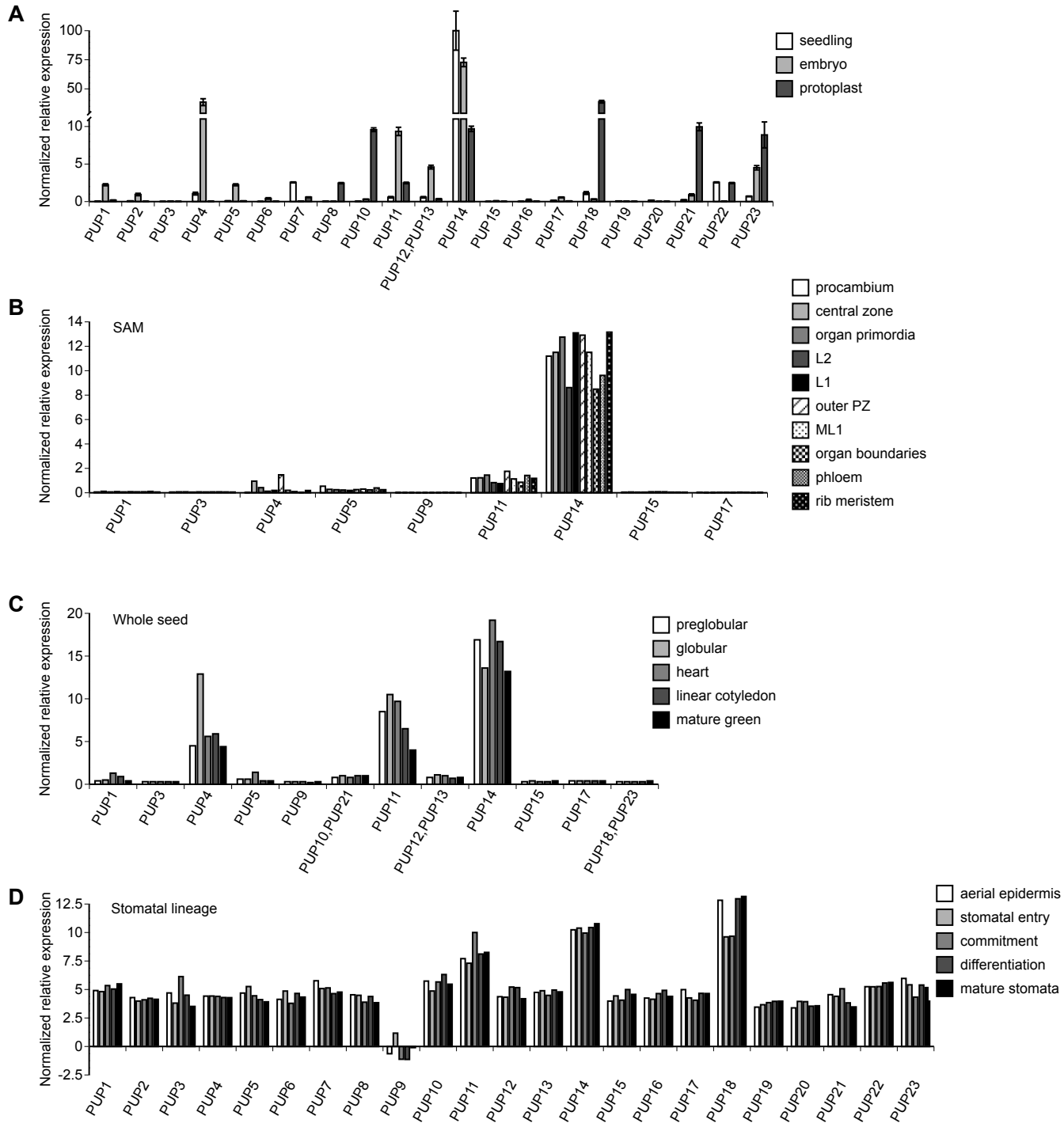

Fig. S1 Conspicuous *PUP14* expression in different developmental contexts.

(A) Transcription profile of all *PUP* family members in seedlings, embryos and mesophyll protoplasts determined by qRT-PCR. (B) Cell type-specific ATH1-based microarray dataset of *PUPs* in the SAM. L1 = layer 1 in SAM, L2 = layer 2, ML1 = layer 1 in meristem and in differentiating organs, PZ = peripheral zone (*11*). (C) ATH1 based microarray dataset of PUPs during seed development (*10*) (D) Stage-specific RNA-seq dataset of *PUPs* in stomatal lineage (*9*). *PUP* AGI identifying numbers: *PUP1*, AT1G28230; *PUP2*, AT2G33750; *PUP3*, AT1G28220; *PUP4*, AT1G30840; *PUP5*, AT2G24220; *PUP6*, AT4G18190; *PUP7*, AT4G18197; *PUP8*, AT4G18195; *PUP9*, AT1G18220; *PUP10*, AT4G18210; *PUP11*, AT1G44750; *PUP12*, AT5G41160; *PUP13*, AT4G08700; *PUP14*, AT1G19770; *PUP15*, AT1G75470; *PUP16*, AT1G09860; *PUP17*, AT1G57943; *PUP18*, AT1G57990; *PUP19*, AT1G47603; *PUP20*, AT1G47590; *PUP21*, AT4G18220; *PUP22*, AT4G18205; *PUP23*, AT1G57980.

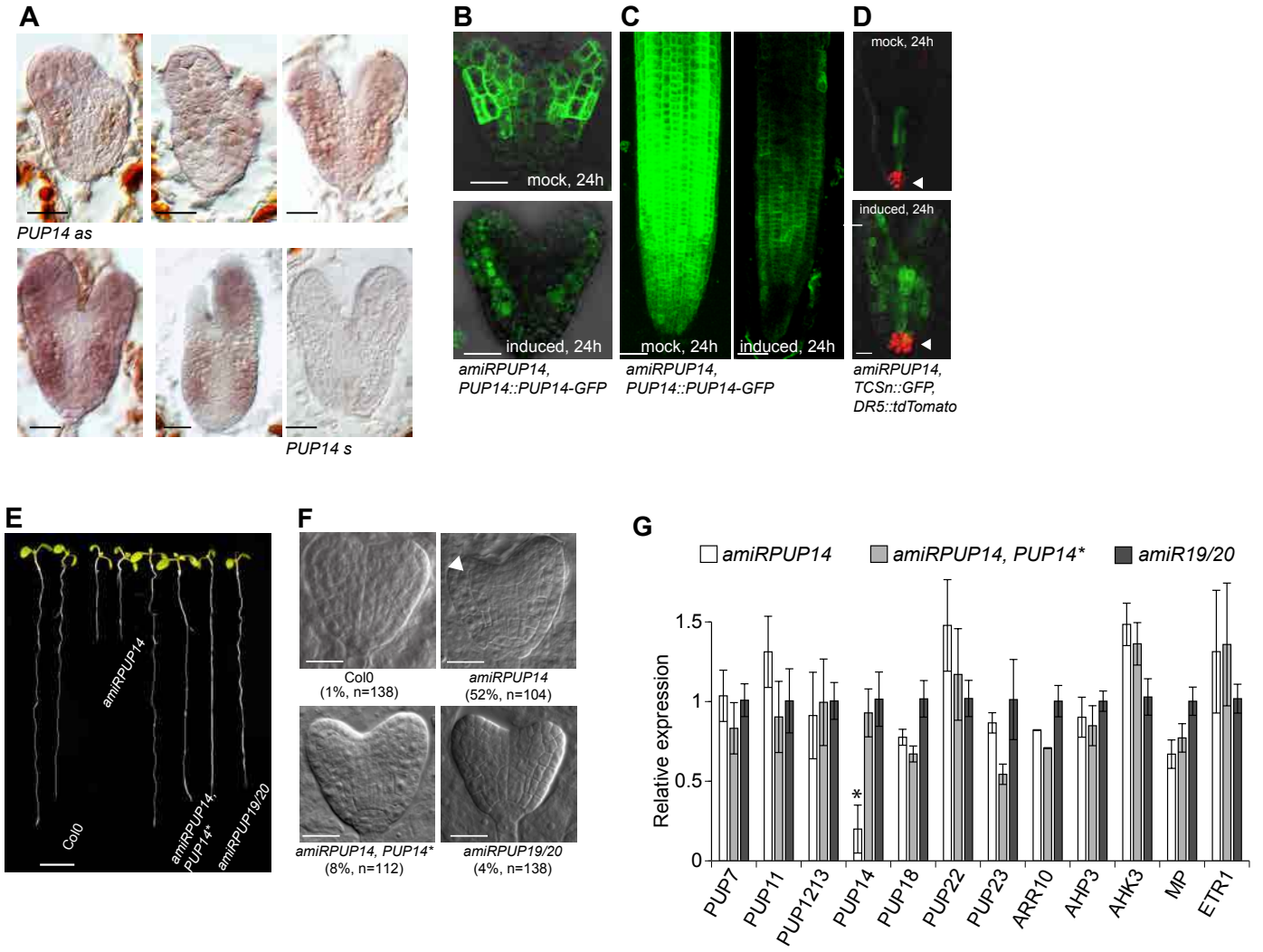

Fig. S2 *amiRPUP14*-induced phenotypes are specific to *PUP14*.

(A) Localization of *PUP14* mRNA in heart and torpedo stage embryos by *in situ* hybridization. First five panels show antisense (as) probe, last panel sense (s) control. (B,C) Decreased PUP14-GFP levels in (B) heart-stage embryos and (C) the seedling root tip after 24 h of *amiRPUP14* induction compared to mock, n=6. (D) *amiRPUP14* affects cytokinin but not auxin response, as shown by unchanged *DR5::tdTomato* (*31*) expression in *amiRPUP14*-induced embryos (arrowheads). Relative fluorescence of tdTomato not affected (unpaired t-test, $p < 0.01$, $n = 5$). (E) Comparison of root growth in Col0, *amiRPUP14*, *PUP14**-complemented and *amiRPUP19/20* seedlings after ethanol induction. (F) Comparison of ethanol-treated embryos of Col0, *amiRPUP14*, *PUP14**-complemented and *amiRPUP19/20* seedlings. (G) Relative transcript levels of *PUP* and unrelated genes in *amiRPUP14; amiRPUP14*, *PUP14** seedlings compared to *amiRPUP19/20*, all ethanol-treated, error bars denote s.e.m. $*P < 0.05$ with one-way analysis of variance with Tukey' HSD post hoc test. Scale bars (A,B,D,F) 20 µm, (C) 50 µm, (E) 1cm.

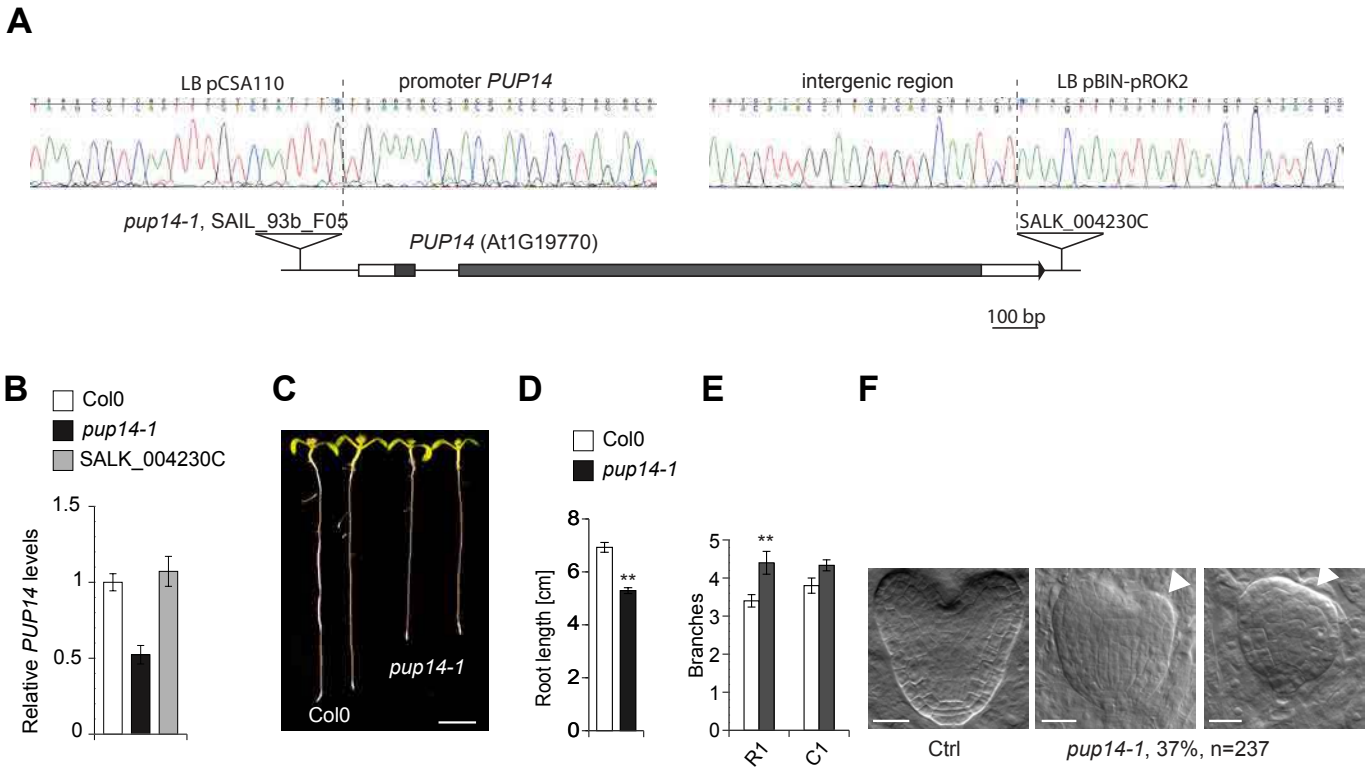

Fig. S3 T-DNA insertion lines at *PUP14* locus.

(A) Sequences of insertion sites of *pup14-1* (SAIL_93b_F03) and SALK_004230C T-DNA insertion lines and schematic representation of insertion sites on gene level. (B) *PUP14* transcript levels in Col0, *pup14-1*, *SALK_004230C*. (C) Root phenotype of *pup14-1* compared to Col0. (D) Quantification of root length of *pup14-1* compared to Col0. (E) Comparison of branch numbers, RI = rosette branches, CI = primary cauline branches, n = 6, **P < 0.01 one-sided *t* test. (F) *pup14-1* embryos show morphological defects in cotyledons and root meristems compared to non-affected siblings from the same silique. Error bars denote s.d. Scale bars 1 cm (C), 20 µm (F).

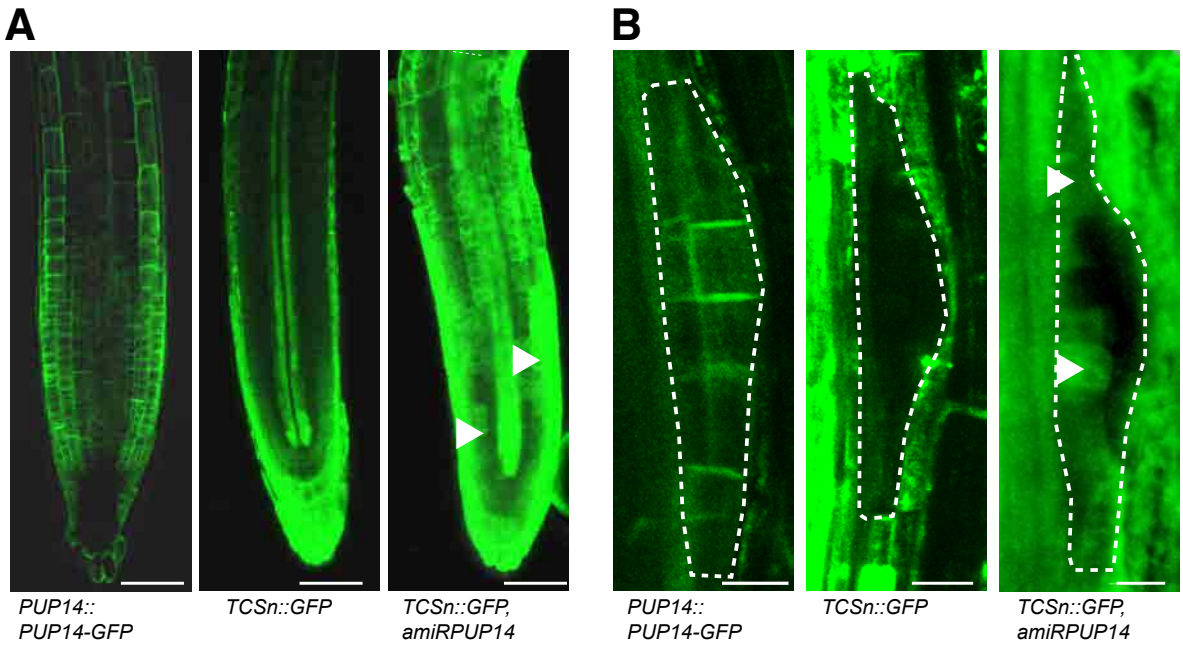

Fig. S4 *PUP14* confines the cytokinin response in seedling roots.

(A) *PUP14::PUP14-GFP* in main root. *TCSn::GFP* in the main root. Ectopic *TCSn::GFP* after 16 h *amiRPUP14* induction (arrowheads) (80 % of roots, n =1 5) roots. (B) LRP, denoted by dotted line. *PUP14::PUP14-GFP*, *TCSn::GFP*, ectopic *TCSn::GFP* (arrowheads) 16 h after *amiRPUP14* induction. Scale bars (A) 50 µm, (B) 10 µm.

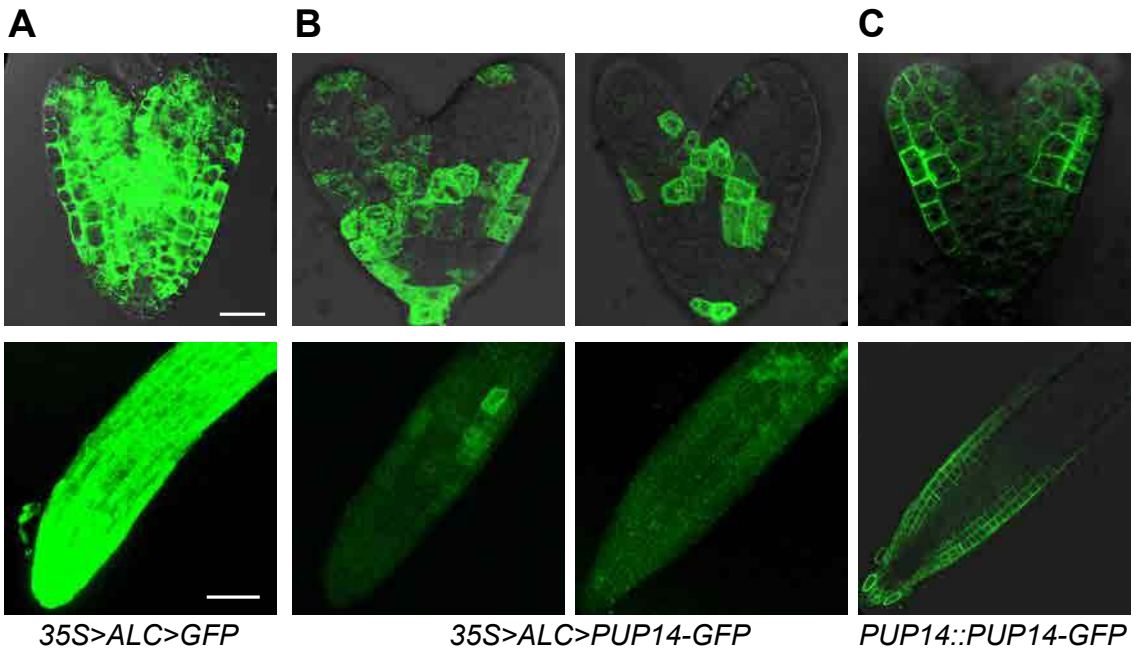

Fig. S5 Ectopic *PUP14-GFP* expression is not well tolerated by plants.

Heart-stage embryos (top panels) and main root apices of 7 d old seedlings (bottom panels) showing (A) 24 h ethanol-induced *35S>ALC>GFP* overexpression, (B) 24 h ethanol-induced *35S>ALC>PUP14-GFP* overexpression and (C) *PUP14::PUP14-GFP* expression. Scale bars 20 µm (top panel), 50 µm (bottom panel).

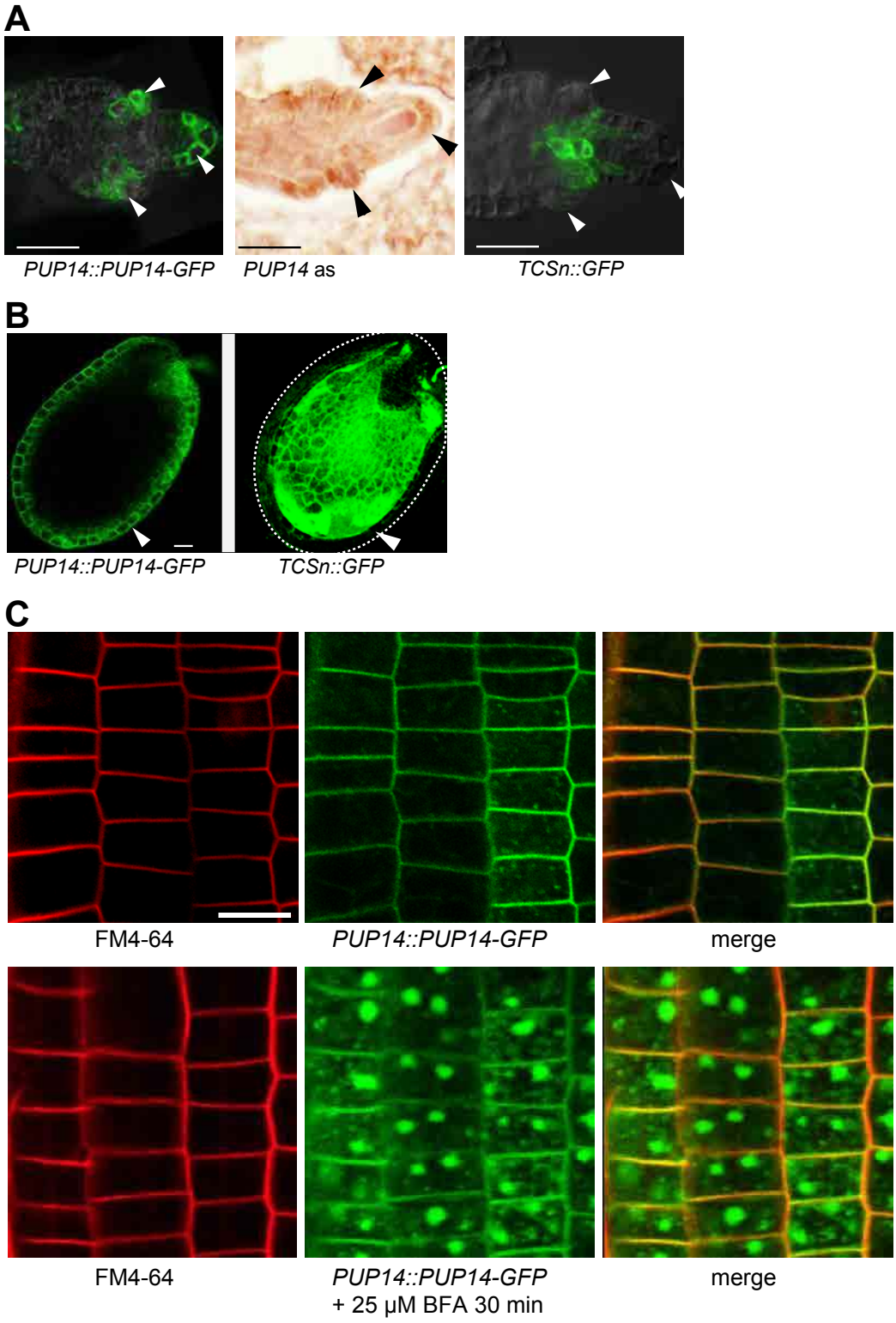

Fig. S6 *PUP14* expression and subcellular localization.

(A,B) *PUP14* expression and cytokinin signaling output in (A) the developing ovule primordium and (B) the seed, detected by reporter transgenes as indicated. In addition, *PUP14* mRNA is detected by in situ hybridization with *PUP14* as RNA probe in (A). Dotted lines delimit the seed coat. Arrowheads indicate peak PUP14-GFP expression levels. (C) PUP14-GFP subcellular localization and trafficking in main root. *PUP14-GFP* colocalization with plasma membrane marker dye FM4-64 (top panels). Addition of the fungal toxin brefeldin A (BFA) causes accumulation of PUP14-GFP signal in vesicles (bottom panels). Scale bars (A,C) 10 µm, (B) 20 µm.

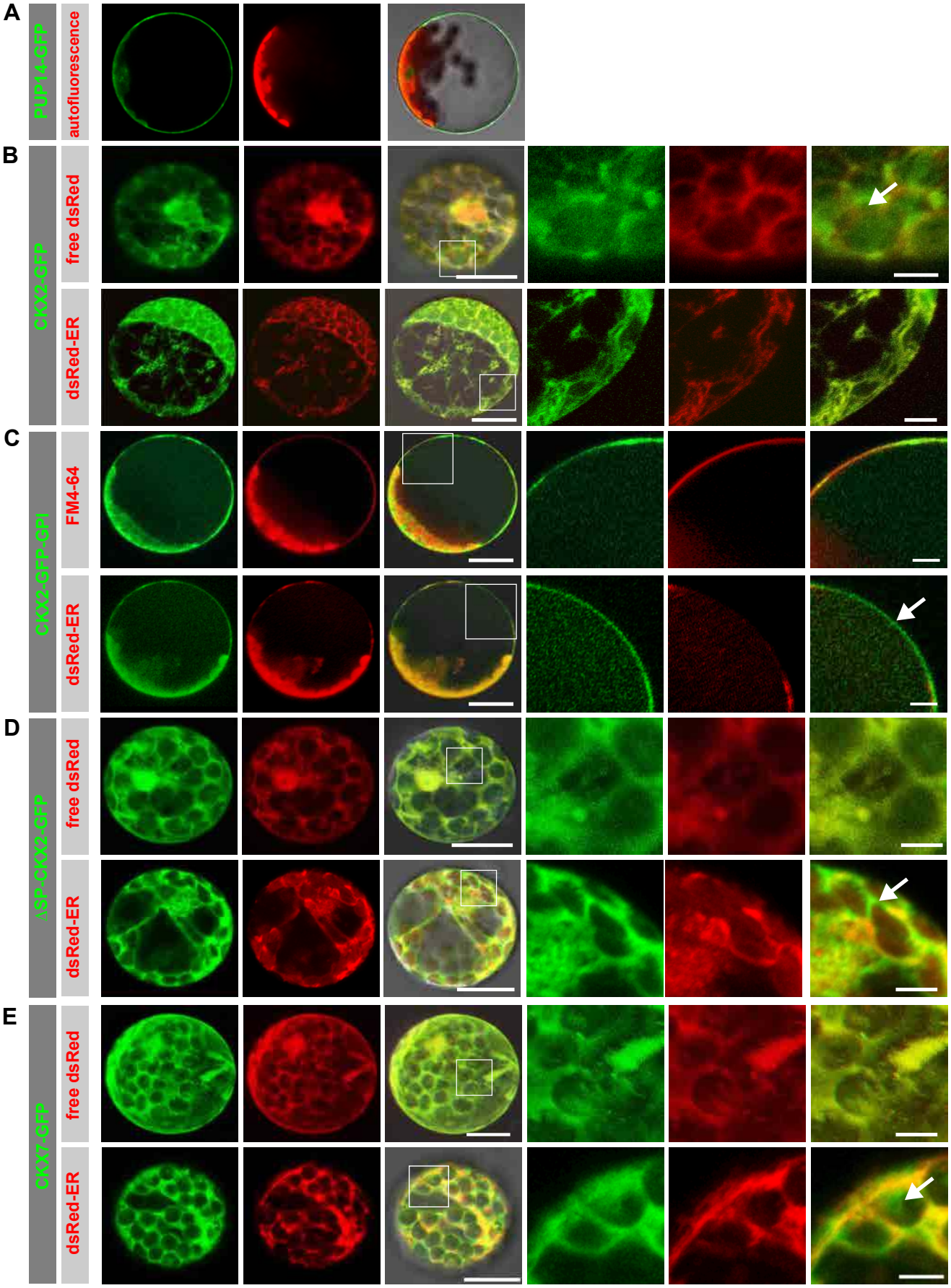

Fig. S7 Subcellular co-localizations of differentially targeted CKX-GFP variants in protoplasts.

(A) Localization of *PUP14-GFP* and (B-E) co-localization of GFP-tagged *CKX* gene products with subcellular markers in protoplasts as indicated. ER labelling with *ER-dsRed*, labeling of cytoplasm with free *dsRed* (*41*), and plasma membrane staining with the lipophilic dye FM4-64. Boxes indicate areas of the enlargement shown to the right. Arrows point to non-overlapping signals. Scale bars 20 μm, in enlargements 5 μm.

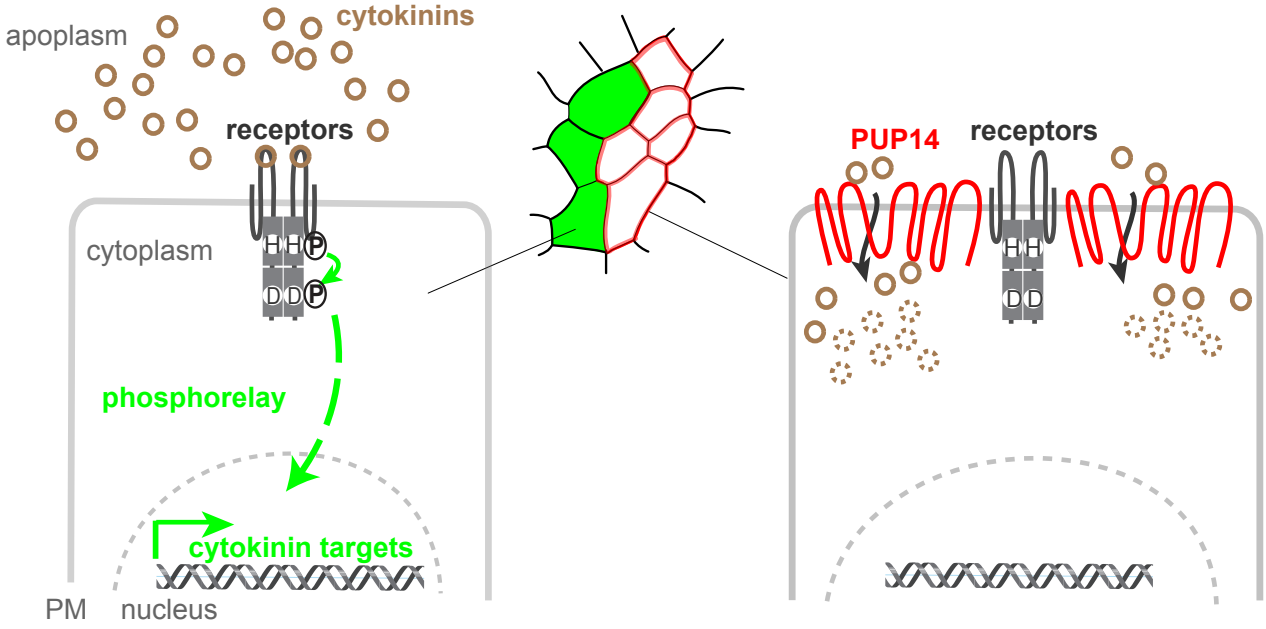

Fig. S8 Model of *PUP14* function in cytokinin signaling.

PUP14 (red) causes the translocation of apoplastic cytokinins to the cytosol, where they are converted to inactive forms (dotted circles). This results in reduced binding to plasma membrane-localized cytokinin receptors, and consequently reduced signaling activation (green denotes cytokinin signaling activity). PM: plasma membrane.

Target gene	Forward primer sequence 5‘ to 3‘	Reverse primer sequence 5‘ to 3‘
eIF4a	TCATAGATCTGGTCCTTGAAACC	GGCAGTCTCTTCGTGCTGAC
ARR5	GGTTGGATTTGAGGATCTGAAG	TCCAGTCATCCCAGGCATAG
ARR6	TTGCCTCGTATTGATAGATGTCTT	CCGAGAGTTTTACCGGCTTC
ARR7	AGATTAAGGAATCTTCAGCATTCAG	CTGCTAGCTTCACCGGTTTC
mGFP	TCAAGGACGACGGGAACTAC	ATCCTGTTGACGAGGGTGTC
PUP1	TGTTTCCGGGAGAAGTTTCA	CGGATTTAAACTCGCCGTAG
PUP2	TCTGTGCATCGTCTCTGGTC	TCTCCTGGAAGCAAATGACG
PUP3	AATACCCGAGACGAGAGACG	CGTCTCTCGTCTCGGGTATT
PUP4	ACCGGAGGTATCTGCATGAC	CACTCCACCAAACACGTCAC
PUP5	TGCAGTCACGTTTCAACTGG	TGACTGTGGATGCCAGAAAC
PUP6	TGCCTGTTCTTGCTGTTGTC	TCTTGGTCTTCTTCTGGCTTTC
PUP7	TTTAGCTATCTGCGGCTTCC	GTGTGACCTTCCTCAACAGG
PUP8	GTCGTGGGACTGATCTTTGAG	GCAATCCCACAGCAGTTATG
PUP10	ACCCACCAGAAGCAGAAGAG	GTAAACTGCGGGACAGCATC
PUP11	TCGACGTATTCGCTCATTTG	GCGGAGAACGACAAGAGAAC
PUP12/13	AGGTTAAGATGGTGGCGATG	TGAGCTTCTCGTGCTCTTTG
PUP14	TCTGTTTCGAGCGTGTTGTC	GCGCTTAAGACGGCAGTAAC
PUP15	GCAGCTGCTCTTAGCGTCTC	TTGTGGATTGGTCATCATCG
PUP16	GTCCGGTTTATTCGCTGATG	AGCACCTCTTCTCTGCCAAC
PUP17	GGCCTAGAATTGGTGCTTTG	TTTGGTTAAGTTCCGCCATC
PUP18	TGCTTTATGTTTCGGGTGTG	CAAAGCCACAAGTGGTGAAG
PUP19	CTGGTAGCTGGGATTCTTGG	AGTTGTTTGGCTTTGGCTTG
PUP20	TTTAGGGCTTGTGGGTCTTG	GCTCCTCCCTTAAACCATCC
PUP21	TTGCACAGGACTGATCTTCG	TGACAGCCAGGATAGGAACC
PUP22	ATCTTGACTTTGGCCTCAGC	GCAGTCCCACAGCAGTTATG
PUP23	TGTGTGCTTCACCACTTATGG	AGCACCAATTCTAGGCCAAC
AT2G32170	TGCTTTTTCATCGACACTGC	CCATATGTGTCCGCAAAATG
AHK3	GGTGGAGTTGGCAGTATACATATC	CGAAACCTCCCAGGATCAC
AHP3	TCTCAGAACTATGAAGGGTGTGTG	AATGTCTTGTACTCAATATCCACTTGC
ARR10	GACACAGGAACAGAGCCAATC	TATGCATGTTCCGAGTGAGC
ETR1	GAGAAGCTCGGGTGGTAGTG	TTTCCAAGACCATCGCTCTC
ARF5/MP	CCCTTCTTCACTCATCTGCTG	TCCATGGGAAGAGTTTGTGG

Table S1.

qRT-PCR primer sequences used in this study.

Name	Purpose	Parent vector	Selection (bacteria/plants)	Insert		
				Primer name	Sequence 5‘ to 3‘	Template
35S>ALC>amiRPUP14_1	Ethanol-inducible binary vector with amiR specific for *PUP14* (variant 1)	*DM7-LIC* (5)	Kan/Kan	LIC-OLIGO_A	tagttggaatgggttcgaaCGACGTTGTAAAACGACGG-CCAG	pRS300
				LIC-OLIGO_B	ttatggagttgggttcgaaCTCGGAATTAACCCT-CACTAAAGG	
				amiR_14_1_I	gaTTATTTGCACAAAGTGTTCTGtctctctttgtattcc	
				amiR_14_1_II	gaCAGAACACTTTGTGCAAATAAtcaaagagaatcaatga	
				amiR_14_1_III	gaCAAAACACTTTGTCCAAATATtcacaggtcgtgatatg	
				amiR_14_1_IV	gaATATTTGGACAAAGTGTTTTGtctacatatatattcct	
35S>ALC>amiRPUP14_2	Ethanol-inducible binary vector with amiR specific for *PUP14* (variant 2)	*DM7-LIC* (5)	Kan/Kan	LIC-OLIGO_A	tagttggaatgggttcgaaCGACGTTGTAAAACGACGG-CCAG	pRS300
				LIC-OLIGO_B	ttatggagttgggttcgaaCTCGGAATTAACCCT-CACTAAAGG	
				amiR_PUP14_2_I	gaTGTTGATAGGTATTTGCACGAtctctctttgtattcc	
				amiR_PUP14_2_II	gaTCGTGCAAATACCTATCAACAtcaaagagaatcaatga	
				amiR_PUP14_2_III	gaTCATGCAAATACCAATCAACTtcacaggtcgtgatatg	
				amiR_PUP14_2_IV	gaAGTTGATTGGTATTTGCATGAtctacatatatattcct	
35S>ALC>amiRPUP19/20	Ethanol-inducible binary vector with amiR specific for *PUP19 and PUP20*	*DM7-LIC* (5)	Kan/Kan	LIC-OLIGO_A	tagttggaatgggttcgaaCGACGTTGTAAAACGACGG-CCAG	pRS300
				LIC-OLIGO_B	ttatggagttgggttcgaaCTCGGAATTAACCCT-CACTAAAGG	
				amiR_19/20_I	gaTTAAAACACGTCCTGCGACGAtctctctttgtattcc	
				amiR_19/20_II	gaTCGTCGCAGGACGTGTTTTAAtcaaagagaat-caatga	
				amiR_19/20_III	gaTCATCGCAGGACGAGTTTTATtcacaggtcgtgatatg	
				amiR_19/20_IV	gaATAAAACTCGTCCTGCGATGAtctacatatatattcct	
PUP14::PUP14-GFP	Reporter	*pCB302 LIC GFP* (Genbank KX510271)	Kan/Basta	PUP14_LICF-F	tagttggaatgggttcgaGCTTCTGCAGTGAAA-GATGTGTT	Col0 genomic
				PUP14_LIC_ GFP302_R	tattggagttgggttcgaaTAAGCCATACGATTGTCTT-TGTG	
hbt::PUP14-GFP; 35S::PUP14	Protoplast expression vector; binary vector for expression in microsomes	*hbt::LIC-GFP*; *pPLV26* (34)	Amp; Kan/Kan	PUP14_LIC_F	tagttggaatgggttcgaATCCATGGCTCAGAATCAA-CAAC	Col0 genomic
				PUP14_LIC_R	ttatggagttgggttcgaaATAAGCCATACGATTGTCTT-TGTG	
PUP14 pCB302	*PUP14* genomic region in binary vector	*pCB302 LIC* (Genbank KX510272)	Kan/Basta	PUP14_LICF-F	tagttggaatgggttcgaGCTTCTGCAGTGAAA-GATGTGTT	Col0 genomic
				PUP14_ LIC3prime_R	ttatggagttgggttcgaaGCACACTTCCAAACATTTTCA	
*PUP14**	*amiRPUP14_2*-resistant *PUP14* in binary vector	*PUP14 pCB302*	Kan/Basta	amiR14_2R* F	CTCTGTTTCTTTTTGCAGAACAATTTGTCCA-GATICCAATAAATA	*PUP14 pCB302*
				amiR14_2R* R	GGTTGAAGAATCACGCTCGATATTTATIGG-AATCTGGACAAATTG	
35S>ALC>PUP14	Ethanol-inducible binary vector (3)	*DM7-LIC* (5)	Kan/Kan	PUP14_LIC_f	tagttggaatgggttcga ATCCATGGCTCAGAATCAA-CAAC	Col0 genomic
				PUP14_LIC_r	ttatggagttgggttcgaa ATAAGCCATACGATTGTCTT-TGTG	
35S>ALC>PUP14-GFP	Ethanol-inducible binary vector (3)	*DM7-LIC* (5)	Kan/Kan	PUP14_LIC_f	tagttggaatgggttcga ATCCATGGCTCAGAATCAA-CAAC	*PUP14::PUP14-GFP*
				GFP_LIC_r	tattggagttgggttcga TTACTTGTACAGCTCGTCCATGC	
35S::PUP1	Binary vector for expression in microsomes	*pPLV26* (36)	Kan/Kan	PUP1_LIC_F	tagttggaatgggttcgaa ACAGCAAGCAGCAAGAAGAA	Col0 genomic
				PUP1_LIC_R	ttatggagttgggttcgaa AGCAACATAATCACTAACAGG-AAG	
hbt::CKX2-HA; hbt::CKX2-GFP	Protoplast expression vector	*hbt::LIC-HA* (Genbank KX510274), *hbt::LIC-GFP* (Genbank KX510273)	Amp	CXX2_LIC_f	tagttggaatgggttcgaaTAAACAAATGGCTAATCTT-CGTT	Col0 genomic
				CXX2_LIC_r	ttatggagttgggttcgaaGATGTCTTGCCCTGGAGATAA-CA	
hbt::ΔSP-CKX2-HA; hbt::ΔSP-CKX2-GFP	Protoplast expression vector	*hbt::LIC-HA* (Genbank KX510274), *hbt::LIC-GFP* (Genbank KX510273)	Amp	CKX2ΔSP_LIC_f	tagttggaatgggttcgaATGATTAAAATTGATT-TACCTAAATCCC	Col0 genomic
				CXX2_LIC_r	ttatggagttgggttcgaaGATGTCTTGCCCTGGAGATAA-CA	

Table S2. Construct list.

Lowercase font in primer sequence denote adaptor sequence, underlined nucleotides indicate mutations or insertions.

Name	Purpose	Parent vector	Selection (bacteria/plants)	Insert		
				Primer name	Sequence 5‘ to 3‘	Template
hbt::CKX7-HA; hbt::CKX7-GFP	Protoplast expression vector	*hbt::LIC-HA* (Genbank KX510274); *hbt::LIC-GFP* (Genbank KX510273)	Amp	CXX7_LIC_f	tagttggaatgggttcgaaCACACACACCAAAATGATAGCT	Col0 genomic
				CXX7_LIC_r	ttatggagttgggttcgaaAAGAGACCTATTGAAAATCTTT-TGACC	
hbt::CKX2-GFP-GPI	Protoplast expression vector	*hbt::LIC-GFP-GPI* (Genbank KX510275)	Amp	CXX2_LIC_f	tagttggaatgggttcgaaTAAACAAATGGCTAATCTT-CGTT	Col0 genomic
				CXX2_LIC_r	ttatggagttgggttcgaaGATGTCTTGCCCTGGAGATAA-CA	
hbt::CKX2-GPI	Protoplast expression vector	*hbt::CKX2-HA*	Amp	GPI_Pst_f	AACGGTGGTTCCCGGTCACAATTCTCATTCGTCG-CCGCCGTGCTCCTCCCTCTTCTTGTCTTTTTCTTC TTCTCTGCCTAActgca	StuI PstI digested *hbt::CKX2-HA*
				GPI_Pst_r	gTTAGGCAGAGAAGAAGAAAAAGACAAGAA-GAGGGAGGAGCACGGCGGCGACGAATGAG-AATTGTGACCGGGAACCACCGTT	

Table S2 (continued).

Construct list. Lowercase font in primer sequence denote adaptor sequence, underlined nucleotides indicate mutations or insertions.